Asymptotic form factors of hadrons and nuclei and the continuity of particle and nuclear dynamics

Stanley J. Brodsky*
Stanford Linear Accelerator Center, Stanford University, Stanford, California 94305

Benson T. Chertok†
American University, Washington, D. C. 20016

(Received 7 June 1976)

The large-q^2 behavior of the elastic form factor of a hadron or nucleus is related by dimensional counting to the number of its elementary constituents. Using the framework of a scale-invariant quark model, dimensional-scaling predictions are derived for the $B(q^2)/A(q^2)$ ratio in the Rosenbluth formula, multiple-photon-exchange corrections, and the mass parameters which control the onset of the asymptotic power law in the meson, nucleon, and deuteron form factors. A simple "democratic chain" model predicts that for large q^2, $F(q^2) \propto (1 - q^2/m_n^{\,2})^{1-n}$, where $m_n^{\,2}$ is proportional to the number of constituents n. In the case of nuclear targets (or systems with several scales of compositeness), we also define the "reduced" form factor $f_A(q^2) = F_A(q^2)/\Pi_{i=1}^{A} F_i(q_i^{\,2})$ in order to remove the minimal falloff of F_A due to the nucleon form factors at $q_i^{\,2} = (m_i^{\,2}/M_A^{\,2})q^2$. Dimensional counting predicts $(q^2)^{A-1} f_A(q^2) \to$ const. A systematic comparison of the data for π, p, n, and deuteron form factors with the dimensional-scaling quark-model predictions is given. Predictions are made for the large-spacelike-q^2 ^{3}He and α-particle form factors. We also relate the deuteron form factor to (off-shell) fixed-angle n-p scattering, and show that the experimental results for $t^5 F_d(t)$ are consistent with the magnitude of the s-wave wave function $u'(0)$ obtained from soft-core potentials. The relation of the dynamics of an underlying six-quark state of the deuteron to the nucleon-potential and meson-exchange-current contributions is discussed. The scaling of $q^2 f_d(q^2)$ implies that the nuclear potential (after removing the effects of nucleon structure) displays the scale-invariant behavior of a theory without a fundamental length scale. Predictions are also given for the structure functions, fragmentation, and large-angle scattering of a nucleus.

I. INTRODUCTION

Measurements of the elastic form factors of the hadrons and nuclei have historically played an essential role in determining the static properties and spatial structure of hadronic matter. In the relativistic domain where $|q^2| \gtrsim O(M^2)$, the classical relationship of the form factor to the Fourier transform of a charge distribution and intuitive concepts such as the use of "body" form factors in the impulse approximation begin to break down, and strictly covariant treatments are required. However, even in the relativistic domain, we can identify the form factor $F(q^2)$ as the probability amplitude for the target to remain intact after absorbing momentum q^μ from a local current. Thus, physically, it is clear that the rate of falloff of $F(q^2)$ will depend on the degree of compositeness of the target as well as the dynamics of the restoring forces. This paper is devoted to an analysis of these relationships, and the implication of present data—particularly the new measurements of the deuteron form factor at large q^2 (see Ref. 1)—to the underlying structure of the hadrons and the nuclear force.

The connection between the asymptotic behavior of the form factor of a bound system and the number n of its constituents is already familiar in many-body Schrödinger theory.[2] In order to transfer momentum to each constituent, the potential must act $n-1$ times. It is straightforward to show that this leads to the large-$\vec{q}^2$ result

$$F_n(\vec{q}^2) \sim \left[\frac{2m}{\vec{q}^2} V(\vec{q}^2)\right]^{n-1} \psi_n^{\,2}(0)\,, \tag{1}$$

where $\vec{q} \sim (1/n)\vec{q}$ is the average momentum transfer to each constituent and

$$\psi_n(0) \equiv \int \prod_{j=1}^{n-1} d^3\vec{k}_j \psi(\vec{k}_j)\,. \tag{2}$$

The derivation assumes that the wave function at relative separation $\vec{x}_j = 0$ is finite. Equation (1) is valid for $m^2 \gg \vec{q}^2 \gg n^2\langle\vec{k}^2\rangle$, where $\langle\vec{k}^2\rangle$ is the mean square momentum of a constituent in the bound state. Taking $V(\vec{q}^2) \sim e^2/\vec{q}^2$ then gives

$$F_n(q^2) \sim \left(\frac{1}{q^2}\right)^{2n-2} \tag{3}$$

for nonrelativistic Coulomb or Yukawa interactions.

The extension of this result to the relativistic domain of the Bethe-Salpeter equation is surprisingly straightforward (see Ref. 3 and Sec. II). The essential change is in the high-energy behav-

ior of V. In the case of quantum electrodynamics, and in fact any renormalizable theory, we have effectively (modulo powers of $\log q^2$ from finite orders in perturbation theory)

$$V(q^2) \sim \frac{e^2}{q^2}\left[1 + O\left(\frac{q^2}{m^2}\right)\right], \tag{4}$$

i.e., $V(q^2)$ becomes constant in the relativistic domain and

$$F_n(q^2) \sim \left(\frac{1}{q^2}\right)^{n-1}, \tag{5}$$

where n is the number of elementary fields (e, μ, γ, q, etc.) which compose the ($l=0$) bound state. This is the prediction of "dimensional counting" which is based on the case of an underlying scale-invariant theory.[3,4]

The predictions based on quark constituents of the hadrons ($|M\rangle = |q\bar{q}\rangle$, $|B\rangle = |qqq\rangle$),

$$\begin{aligned} &q^2 F_\pi(q^2) \to \text{const}, \\ &(q^2)^2 F_p(q^2) \to \text{const}, \end{aligned} \tag{6}$$

appear to be consistent for spacelike q^2 larger than the square of the mass of the respective hadrons (see Figs. 1 and 13). The measurements of $F_\pi(q^2)$ for timelike $t \equiv q^2$ from $e^+e^- \to \pi^+\pi^-$ also agree with the predicted behavior as in Ref. 3 and Fig. 6. Further, and perhaps most remarkably, the dependence of the elastic deuteron form factor measured in Ref. 1 is consistent with the approach of $t^5 F_d(t) \to$ const predicted for a six-quark state (see Figs. 1 and 9). This was the impetus for the present investigation.

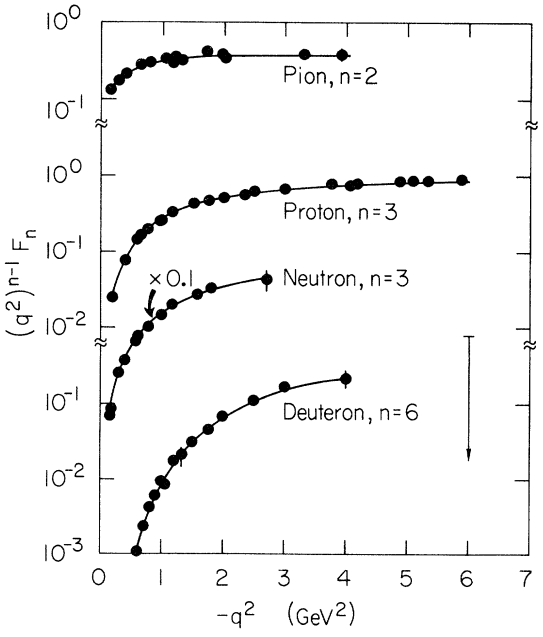

FIG. 1. Elastic electromagnetic form factors of hadrons for large spacelike q^2 in terms of the dimensional-scaling quark model. The curves simply connect the data points. (The neutron data have been multiplied by 0.1.)

If the target has spin, then the scaling law, Eq. (5), is the prediction for the leading form factor $A^{1/2}(q^2)$ in the Rosenbluth formula

$$\frac{d\sigma}{d\Omega} = \left(\frac{d\sigma}{d\Omega}\right)_{\text{Mott}}\left[A(q^2) + B(q^2)\tan^2\tfrac{1}{2}\theta_L\right], \tag{7}$$

and further, $B(t)/A(t) \to -t/2M^2$ if the elementary charged constituents have spin $\frac{1}{2}$. For the nucleon, this implies dominance of the Dirac form factor

$$\frac{t}{4M^2} F_2^2(t)/F_1^2(t) \to 0. \tag{8}$$

We also show (see Sec. II A) that multiple photon exchange can give a correction of order $Z\alpha$ to the asymptotic large-t cross section.

At first sight, it may seem surprising that the dynamics of any system as complex as the deuteron can be related to the dynamics of a six-quark state. However, to the accuracy of present knowledge, the electromagnetic interactions of hadrons (e.g., Bjorken scaling of deep-inelastic lepton scattering, current algebra, e^+e^- annihilation) are described by quark currents, and the spectroscopy of hadrons and the quantum flow of the strong interactions can be identified with the underlying skeletal substructure of the quark diagrams. Models of the hadronic interactions, including quark-gluon gauge theories, thus imply a microscopic description of the nuclear force and lead to constraints on its short-distance behavior. Of course, since asymptotic quark states have not been found, there must be an equivalent or "dual" description in terms of normal hadronic states. In fact, it is this complementarity or mathematical equivalence which, as we shall see, leads to important constraints on the meson-exchange contributions to the nuclear force at short distances and exchange-current contributions to the deuteron form factor.

The physical picture which underlies the dimensional-counting prediction, Eq. (5), is that, at large q^2, binding corrections are negligible and can be set equal to zero. The scaling of the form factor then has the same short-distance scaling behavior as that of the amplitude for an electron scattering on n on-shell constituents, each with a finite share of the initial and the final momentum (see Sec. II A). In the case of renormalizable theories with dimensionless coupling constants and no intrinsic length scale at short distances, Eq. (5) is then obtained—modulo logarithmic corrections of the same order expected to Bjorken

scaling of deep-inelastic scattering.[3] Empirically, these corrections seem to be small and will be neglected for the range of q^2 discussed here.

The deuteron form factor will be discussed from several points of view within an equipartition picture in this paper. In Sec. II D we use the simplest quark diagrams [the cascade model, as in Fig. 2(a)] as an illustration of how the mass parameters which control the onset of asymptotic scaling in the meson, nucleon, and deuteron form factors can be related. A phenomenological discussion of the new large-q^2 data on the deuteron, considered together with comparable data for the pions and nucleons, is then presented.

In the case of quark models such as quantum chromodynamics, the simple cascade diagram is first-order forbidden, and an interchange of quarks between the nucleons is required. It is an interesting question whether this effect can be distinguished phenomenologically in the large-q^2 form factor. The relationship of quark-interchange diagrams to the exchange-current contributions is discussed in Sec. II D.

The structure of the deuteron form factor in a relativistic theory can also be understood in some detail from Fig. 2(b). If we neglect the nuclear binding, then the calculation of the form factor requires each nucleon to absorb momentum transfer $\sim\frac{1}{2}q^\mu$. Thus it is natural to define the "reduced" form factor of the deuteron,

$$f_d(q^2) \equiv \frac{F_d(q^2)}{F_N^2(q^2/4)}\,, \tag{9}$$

where the two powers of the nucleon form factor remove in a minimal way the effects of nucleon structure. $f_d(q^2)$ is displayed from existing data in Fig. 3. In a sense, the reduced form factor contains the essential dynamics of the nuclear interaction, and it can be directly related to the exchange-current contribution of standard analyses. Using dimensional counting, Eq. (5), we predict for large q^2 (Ref. 5)

$$f_d(q^2) \to \frac{\text{const}}{q^2 - m_0^2}\,. \tag{10}$$

A comparison of the prediction $(1 - q^2/m_0^2)F_D(q^2)/F_N^2(q^2/4) \to$ const with the data of Ref. 1 is shown in Fig. 9. (The value $m_0^2 = 0.28$ GeV^2 is predicted from the parametrization of the pion form factor.) The (roughly) constant behavior of $(q^2 - m_0^2)f_D(q^2)$ in Fig. 9 for $|q^2| \gtrsim 0.7$ GeV^2 appears to be a striking success for the quark-counting approach. This premature onset of scaling appears to be a general feature of electromagnetic interactions of hadrons. As we discuss in Sec. II C, the scaling of $q^2 f_D(q^2)$ implies that the nuclear potential (after removing the effects of nucleon structure) at momentum

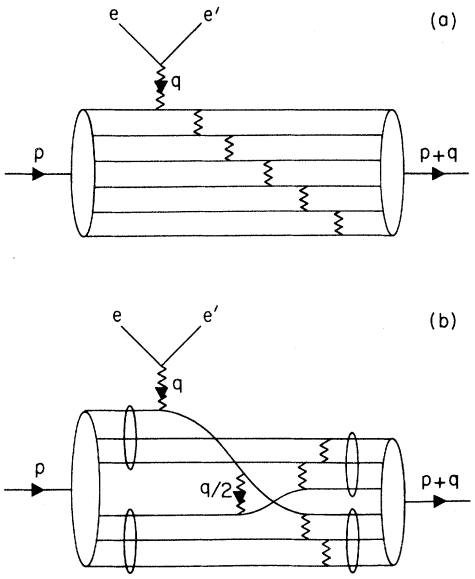

FIG. 2. Two possible quark-constituent views of e-D elastic scattering are (a) the democratic chain (cascade) model and (b) the quark-interchange model.

transfers beyond ~0.7 GeV displays the scale-invariant behavior of a renormalizable interaction, i.e., V = const as in Eq. (4). The constraints on the exchange-current contribution and the generalizations to other nuclei, in particular with pre-

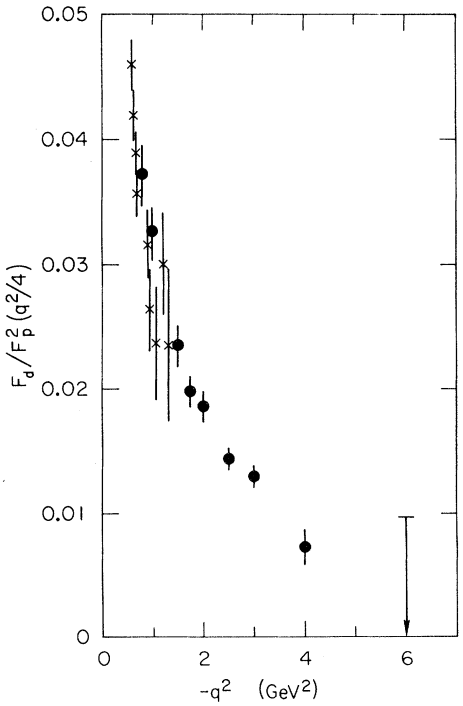

FIG. 3. "Reduced deuteron form factor," f_D versus $-q^2$. The data are from Ref. 26 (×) and Ref. 1 (●).

dictions for ^{3}He and ^{4}He, are also discussed in Secs. II and IV.

The deuteron form factor can also be predicted from the behavior of off-shell nucleon-nucleon scattering near $\theta_{\text{c.m.}} = \pi/2$. The deuteron wave function at the origin, $\psi_D(0)$, is then evaluated using both sets of experimental data. This is discussed in Sec. II C. We also discuss other nuclear tests sensitive to short-distance interactions in Sec. VI.

This paper is organized as follows. The scaling laws are developed in Sec. II, relating (a) fixed-angle scaling to elastic form factors, (b) reduced form factors for general composite systems to dimensional scaling laws, (c) the deuteron form factor to n-p elastic scattering at fixed angle, and (d) binding corrections in a dimensional-scaling quark picture to elastic form factors. The data set of elastic form factors for π, p, n, and d is presented in Sec. III. The systematic comparison of these data with the dimensional-scaling quark-model predictions developed in Sec. II is made in Sec. IV. The results of this investigation are summarized in Sec. V, followed by the conclusions in Sec. VI which generalize on the continuity between nuclear and particle physics. The partition method for bound-state calculations is reviewed in Appendix A. Appendix B contains a discussion of the proton elastic-form-factor data and phenomenology, and Appendix C contains predictions for the neutron form factors.

II. SCALING LAWS

A. Fixed-angle scattering laws and form factors

If the binding interactions of a composite system are sufficiently well behaved, then at large momentum transfers binding corrections can be ignored and effectively the bound-state scattering amplitude is proportional to the on-shell multiparticle amplitude $\mathfrak{M}_N$ obtained by partitioning the momentum of each hadron among its constituents. As discussed in Appendix A and Ref. 3, the required condition for this to be valid is that the wave function be finite at relative distance $x_\mu = 0$. In the case of constituent spin, the spinor factors, u, v, etc., are included in $\mathfrak{M}_N$. We note that the amplitude has dimensions $[L]^{N-4}$.

In the scale-invariant theory where, asymptotically, only the invariants t and $s = E_{\text{c.m.}}^2$ set the mass scale, we have $\mathfrak{M}_N \sim t^{(1/2)(4-N)} g(t/s)$ and thus

$$\frac{d\sigma}{dt}(A+B \to C+D) \to \frac{1}{t^{N-2}} f(t/s)\,, \tag{11}$$

where N is the total number of elementary fields in A, B, C, D. The applications of Eq. (11) to fixed-c.m.-angle hadron-hadron scattering are discussed in Ref. 3. Electron-hadron scattering is a special case of Eq. (11):

$$\frac{d\sigma}{dt}(eH \to eH') = \frac{4\pi\alpha^2}{t^2} F_H^{\,2}(t) f(t/s)\,, \tag{12}$$

where $F_H(t) \to \text{const}/t^{n_H - 1}$. In fact the fixed-angle scaling law holds to any finite order in α. Thus the two- (or higher-) photon-exchange contributions also scale and simply give a correction of order α to $f(t/s)$, in agreement with the explicit calculations of Gunion and Stodolsky.[6] Comparing Eq. (12) with the Rosenbluth formula we have, in order α, the predictions

$$[A(t)]^{1/2} \to \frac{\text{const}}{t^{n_H - 1}} \tag{13}$$

and

$$\frac{B(t)}{(t/M^2)A(t)} \to \text{const (or zero)}\,. \tag{14}$$

($B \equiv 0$ for a spinless target.) More specifically, we assume the angular dependence of $d\sigma/dt$ will reflect the angular distribution of the elementary scattering of the electron on the charged constituents. For spin-$\frac{1}{2}$ constituents, we thus have the further prediction

$$B(t) \to \frac{-t}{2M^2} A(t)\,. \tag{15}$$

Alternately, we can use the exclusive-inclusive connection which ensures continuity between the elastic and inelastic electron scattering cross sections. The condition (15) is equivalent to the Callan-Gross relation $R = \sigma_L/\sigma_T \to 0$ at $x = -q^2/2p\cdot q \to 1$. More generally, continuity at $x = 1$ requires that

$$\frac{B(t)}{A(t)} \Rightarrow \frac{2W_1}{W_2}\bigg|_{x=1} = \frac{2}{1+R}\left(\frac{\nu^2 - t}{-t}\right)\bigg|_{x=1} = \frac{-t}{2M^2}\,\frac{(1 - 4M^2/t)}{1+R}\,, \tag{16}$$

where M is the target mass. The measured value of R for the proton at large x is $\sim 0.10 \pm 0.05$ for $|t| \geq 2$ GeV^2.[7]

B. The reduced form factor

The partition model also leads to simple predictions for nuclear targets or general systems with a series of scales of compositeness. Thus, consider a composite of A constituents each with an on-shell form factor $F_i(t)$. In the limit where binding can be neglected, each constituent absorbs momentum $(m_i/M_A)q$. Thus, it is natural to define the "reduced" form factor

$$f_A(t) = \frac{F_A(t)}{\prod_{i=1}^{A} F_i\left((m_i^{\,2}/M_A^{\,2})t\right)}\,, \tag{17}$$

which removes the minimal falloff of the form factor due to constituent structure. It is clear physically that $f_A(t)$ should be a decreasing function of t since one still has to pay a penalty for keeping A intact. Using dimensional counting, i.e., an underlying scale-invariant theory, we have from Eqs. (5) and (17)

$$f_A(t) \to \frac{\text{const}}{t^{A-1}} . \tag{18}$$

Thus the reduced form factor is predicted to have the same falloff as a corresponding bound state of elementary constituents. (Note that only $I=0$ states are considered here). In particular, $f_D(t)$ and $f_{^3\mathrm{He}}(t)$ are predicted to have the same monopole and dipole falloff as the mesons and baryons, respectively. These and other predictions are summarized in Table I. Note that in each case F refers to the $\sqrt{A}$ form factor in the Rosenbluth formula. We emphasize that the usual definition of a "body" form factor $f_A^{\text{body}}(t) = F_A(t)/F_p(t)$ has no natural significance in a relativistic theory.

C. The deuteron form factor and fixed-angle *n-p* scattering

If the deuteron nuclear wave function $\psi_D(x)$ is finite at $x_\mu = 0$, then the calculation of the large-q^2 limit of the deuteron form factor is equivalent to the calculation of the amplitude for the process

$$\gamma_V(q^2) + p + n \to p' + n' ,$$

where the initial nucleons each have 4-momentum $p/2$ and the final nucleons have 4-momentum $(p+q)/2$, i.e., binding energy $\to 0$. Thus, as seen in Fig. 4, $F_d(q^2)$ has the structure

$$F_d(q^2) \sim 2\Gamma(q^2)\Delta(q^2/2)T(q^2)\psi_D^2(0) , \tag{19}$$

where the coupling of the nucleon to an off-shell state with mass squared $\mathfrak{M}^2 = q^2/2$ is given by the vertex function $\Gamma(q^2)$, the off-shell nucleon propagator is $\Delta(\mathfrak{M}^2)$, and

$$T(q^2) = T(t = q^2/4, u = q^2/4, \mathfrak{M}^2 = q^2/2)$$

is the connected n-p scattering amplitude for 90° scattering with one-nucleon leg off-shell.

In fact, we can argue—from the observations of Bjorken scaling in deep-inelastic scattering or $e^+e^- \to N + X$—that $\Gamma(q^2)\times\Delta(q^2/2)$ is scale-invariant, i.e., at large q^2

$$\Gamma(q^2)\Delta(q^2/2) \sim \frac{1}{q^2/2} , \tag{20}$$

the same scaling as in free-field theory.[8] This result is of course also evident in the quark model. Thus

$$F(q^2) \sim 2\frac{1}{q^2/2} T(q^2)\psi_D^2(0) , \tag{21}$$

and the asymptotic behavior of $F(q^2)$ is controlled directly by the large $t=u$ behavior of the off-shell n-p scattering amplitude.

In the case of *on-shell* proton-proton and neutron-proton scattering, the fixed-$\theta_{\text{c.m.}}$ cross section fits the form[9]

$$\frac{d\sigma}{dt} = \frac{1}{16\pi s^2}|T|^2 = \frac{f(\theta_{\text{c.m.}})}{s^n} \tag{22}$$

with $n = 9.7 \pm 0.5$ for $pp \to pp$, $|t|, |u| \gtrsim 2$ GeV^2. (The dimensional-counting prediction is $n = 10$.[3]) Thus, at 90° $T \propto s^{-3.85\pm0.25}$. Further, it is easy to see from field-theory calculations in perturbation theory that the extrapolation of T from on-shell to the off-shell *spacelike* mass $\mathfrak{M}^2 = q^2/2 < 0$ can only *decrease* the amplitude. Thus we obtain an upper bound to the asymptotic behavior of F_D:

$$F_d(q^2) \leq \frac{C}{(q^2)^{4.85\pm0.25}} . \tag{23}$$

We can, in fact, go one step further. For general sets of field-theory graphs[10] it is straightforward to show that the scaling behavior $T(q^2) \propto (q^2)^{-n}$ for $t = u = q^2/4$ is unchanged by the extrapolation from on-shell to spacelike $\mathfrak{M}^2 = q^2/2$. Thus we can predict directly from the Bjorken scaling behavior of deep-inelastic scattering and the observed fixed-angle scaling behavior of fixed-angle nucleon-nucleon scattering the large-q^2 result

$$F_d(q^2) = \frac{C}{(q^2)^{4.85\pm0.25}} , \tag{24}$$

in agreement with the interpretation of the mea-

TABLE I. Compositeness of matter.

Bound state	$F_i\left(\frac{m_i^2}{m_A^2}t\right)$	Number of constituents	$f_A(t)$
e, μ, γ, q	1	1	t^0
π, K	1	2	t^{-1}
p, n	1	3	t^{-2}
D	$F_p(t/4)$	2	t^{-1}
^{3}He	$F_p(t/9)$	3	t^{-2}
^{4}He	$F_p(t/16)$	4	t^{-3}

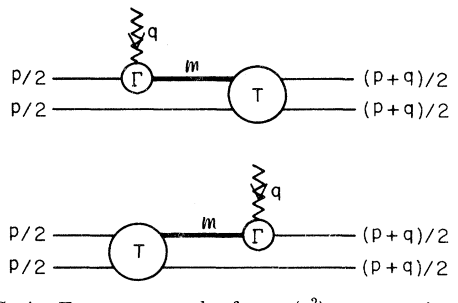

FIG. 4. Feynman graphs for $\gamma_V(q^2) + p + n \to p' + n'$.

surements of Ref. 1 as, e.g., in Fig. 9.

It is of interest to see whether we can understand the order of magnitude of the constants entering the form-factor calculation. The large-t on-shell 90° n-p scattering amplitude fits the approximate form $T\sim 5\times 10^3\ \mathrm{GeV}^8/t^4$. For the off-shell continuation we shall assume the form

$$T(q^2)\sim \frac{5\times 10^3\ \mathrm{GeV}^8}{t^2(t+\mathfrak{M}^2)^2} \sim \frac{1.5\times 10^5\ \mathrm{GeV}^8}{(q^2)^4}\ , \tag{25}$$

which is suggested by extrapolations of off-shell form factors.[11] Using Eq. (21), we then have

$$\psi_{\mathrm{nr}}{}^2(0)\cong 2M_p\psi_D{}^2(0)=\frac{M_p q^2 F_D(q^2)}{2T(q^2)} \cong \frac{(q^2)^5 F_D(q^2)}{3\times 10^5\ \mathrm{GeV}^7}\ . \tag{26}$$

Taking $(q^2)^5F_D(q^2)\sim 1\ \mathrm{GeV}^{10}$ from Fig. 9 gives

$$u'(0)=\sqrt{4\pi}\,\psi_{\mathrm{nr}}(0)\sim 0.1 m_\pi{}^{3/2}\ , \tag{27}$$

which is of the order of magnitude of the s-wave wave function [normalized to $\int_0^\infty u^2(r)dr=1$] obtained for the soft-core potentials.[12]

Notice also that consistency between the asymptotic scaling laws for $T(q^2)$ and $F(q^2)$ requires $u'(r)$ to be nonzero at $r\to 0$. *Thus there is no "hard core" in the effective nucleon-nucleon potential—at least for the range $r\gtrsim 1/Q_{\max}\sim 0.06/m_\pi$ (0.08 F) probed thus far in the deuteron form-factor measurements.*

It should also be noted that $V_{\mathrm{eff}}(q^2)\equiv 2M_pT(q^2)$ is the effective nucleon-nucleon potential in the two-body Schrödinger theory. As we have seen, the asymptotic falloff of $T(q^2)$ is consistent with the $(q^2)^{-4}$ behavior of $F_N{}^2(q^2/4)$. Thus the entire falloff of the effective potential can be understood to be due to just the dynamical structure of the nucleons themselves, with *no additional falloff from the exchange force*. The scaling behavior for the "reduced" amplitude

$$t(q^2)=\frac{T(q^2)}{F_N{}^2(q^2/4)}\sim \mathrm{const} \tag{28}$$

is in fact (modulo logarithmic terms) exactly what is expected in underlying theories which are scale-invariant at short distances, including quantum electrodynamics (in perturbation theory) and gauge theories with asymptotic freedom.

D. Quark description of form factors

Within the accuracy of our present knowledge, the electromagnetic interactions of hadrons can be described by quark currents. The empirical evidence has been mentioned in the Introduction. The recent observation of jets with the angular distribution appropriate to e^+e^- annihilation to pointlike fermions is particularly striking. These results, taken together with hadron spectroscopy, imply that hadrons have a finite composite structure with the degrees of freedom of the quark model. The form-factor calculations thus require the rearrangement of a finite number of elementary constituents and yield power-law falloff, $t^NF(t)\to \mathrm{const}\neq 0$. In constrast, bootstrap or continuum models with a uniform current distribution imply an infinite-composite hadronic structure and exponentially damped form factors.[2,13]

More specifically, if the hadronic wave function is finite at zero relative separation, binding corrections can be neglected at large momentum transfer (see Appendix A and Sec. II A), and the calculation of the asymptotic form factor is equivalent to the calculation of the amplitude $\mathfrak{M}_n$ for rearranging the n-constituent quarks parallel to p^μ to the final $p^\mu+q^\mu$ direction. This result holds for nuclei at large q^2 as well as for the usual hadrons. If the quarks are structureless and the interactions are scale-free then this leads to the dimensional-counting prediction $t^{n-1}F(t)\to$ const. We note that if deviations from Bjorken scaling are found at large q^2—as might be due to quark substructure[14]—then the dimensional-counting prediction applies to the reduced form factor

$$f_{q/A}(q^2)\equiv \frac{F_A(q^2)}{\prod_{i=1}^{n} F_q(q_i{}^2)} \tag{29}$$

($q_i=x_iq$, $\sum_{i=1}^n x_i=1$) obtained after removing the quark-form-factor dependence.

It is an important and interesting question whether the mass parameters in the various hadronic form factors can be related. The mass scales which determine the preasymptotic form of $F(t)$ clearly will depend in detail on the binding parameters and internal masses of the constituents. In the case of nonstrange hadrons, the quark masses are usually assumed to be small compared to their average transverse momentum in the bound-state wave function. In the models described below we shall assume that the essential mass scale which enters the scattering amplitude and propagators is the mean transverse momentum $\langle k_\perp{}^2\rangle^{1/2}$, which we take as a hadron-independent constant. We recall that this mean transverse momentum, which is a general observable in high-energy collisions where $\langle \vec{k}_\perp\rangle\sim 300$ to 400 MeV, determines the large $q^2, q\cdot p$ kinematic boundary where Bjorken scaling sets in. The convergence of the integrals at large transverse momentum is guaranteed by the condition on the

Bethe-Salpeter wave function $\psi(0)<\infty$.

Even if we assume a specific quark-gluon field theory, the complete calculation of the hadronic form factors is a formidable task. All diagrams contribute to the quark-scattering amplitude $\mathfrak{M}_n$ in the resonance regions ($t\sim m_\rho{}^2$, etc.) and to the leading asymptotic power behavior—modulo logarithms. However, in asymptotic-freedom gauge theories such as quantum chromodynamics, the coupling constant α_s is not very large ($\alpha_s\sim 0.3$) for $q^2\gtrsim\langle\vec{k}_\perp{}^2\rangle$, and decreases slowly with q^2. Thus we can hope to calculate at least the rough structure of the nonresonant contributions from the lowest perturbation theory contributions. We can then assume that the diagrams in lowest-order perturbation theory for $\mathfrak{M}_n$ give the leading asymptotic behavior. Since we are interested only in identifying the leading power dependence here, we can ignore the slow logarithmic corrections from higher-order loop diagrams and the dependence of $\alpha_s(q^2)$. As discussed in Ref. 3, the logarithms in an asymptotic-freedom theory arising from the ultraviolet region do not accumulate to change the effective power behavior. Further, the infrared singularities cancel for neutral (color-singlet) composite systems.

The computation of the complete gauge-invariant set of Born diagrams for $\mathfrak{M}_n$ can be readily carried out in any renormalizable theory. It is easy to show that for large q^2 the gluon propagator is always compensated by its couplings to the quark currents, leaving only a net falloff $(q^2)^{-1}$ for each quark propagator. The asymptotic falloff of $\mathfrak{M}_n$ then gives the dimensional counting result $(q^2)^{n-1}F(q^2)\to$ const. However, it is of interest to study the structure of the Born-approximation diagrams further in order to see how the sharing of the momentum transfer controls the mass scale for the onset of the asymptotic predictions.

We shall assume that, on the average, the momentum of the hadrons is partitioned equally among its constituents, $p_i=x_ip+\kappa_i$, where $x_i=m_i/M=1/n$ and $|\kappa_i{}^2|=\beta^2$ is the mean square of the quark momentum in the rest frame of the hadron. As an illustration of the way in which the mass parameters enter the form-factor calculations, we compute the amplitude for any of the simple "democratic" chain diagrams in which no quark interacts more than twice. For such graphs [see Fig. 2(a)], after spin traces and rationalizing denominators, the quark propagators give

$$F_n(q^2)\propto\prod_{j=1}^{n-1}\left[\left(\frac{p}{n}+\frac{j+1}{n}\,q+\kappa_j\right)^2-m_j{}^2+i\epsilon\right]^{-1}\sim\prod_{j=1}^{n-1}\left[\beta^2-\frac{j(j+1)}{n^2}\,q^2\right]^{-1}. \tag{30}$$

(Note that the $q\cdot\kappa_j$ term, averaged over the angle, has the same effect as the $\kappa_j{}^2$ term). We incorporate all finite-mass corrections to the quark propagator in the constant β^2.

In the case of spin-$\frac{1}{2}$ quarks, the effective gluon interaction is ($q_j=[(j+1)/n]\,q$)

$$V_j(q^2)\sim\frac{1}{q_j{}^2-\lambda^2+i\epsilon}\,[q_j{}^2+O(m_j{}^2)+O(\kappa_j{}^2)]\ , \tag{31}$$

which leaves the asymptotic form of $F_n(q^2)$ unchanged.

Although Eq. (30) is approximate, it is representative of the structure of the contributions to the form factors at large q^2, and gives a clue to how the mass parameters of the various form factors are interrelated. For the mesons and nucleons, the off-shell quark propagators give (for large q^2)

$$F_M(q^2)\sim\frac{C_M}{1-\frac{1}{2}q^2/\beta^2}\ , \tag{32}$$

$$F_N(q^2)\sim\frac{C_N}{(1-\frac{2}{3}q^2/\beta^2)(1-\frac{2}{9}q^2/\beta^2)}\ , \tag{33}$$

where we have assumed that the average momentum of the quarks within hadrons (and the average transverse momentum $\langle\vec{k}_\perp{}^2\rangle\sim\frac{2}{3}\beta^2$) is universal. Equations (32) and (33) should be indicative of the leading mass corrections to the asymptotic behavior. We also note that for the leading correction (to order β^2/q^2) Eq. (30) is equivalent to

$$F_n(q^2)=C_n\left(\frac{1}{1-q^2/m_n{}^2}\right)^{n-1}\ , \tag{34}$$

where

$$m_n{}^2=\beta^2\frac{n^2}{n-1}\sum_{j=1}^{n-1}\frac{1}{j(j+1)}\equiv n\beta^2\ , \tag{35}$$

which shows how the mass scale increases as q^2 is distributed among an increasing number of constituents.

Numerically, the best fit to $F_\pi(q^2)$ for spacelike q^2 is

$$F_\pi(q^2)=[1-q^2/0.471(\pm0.010)\ \text{GeV}^2]^{-1}$$

(see Ref. 15), implying that $\beta^2=0.235\ \text{GeV}^2$ and that $\langle k_\perp{}^2\rangle^{1/2}\sim 400$ MeV. Using Eq. (34), this gives for the large-q^2 nucleon form factor

$$F_N(q^2)\sim\frac{C_N}{(1-q^2/0.71\ \text{GeV}^2)^2}\ . \tag{36}$$

Thus we can obtain a rather simple understanding of the relationship of the meson form factor to the "canonical" empirical dipole fit to the nucleon form factor and the origin of the constant $3\beta^2=0.71\ \text{GeV}^2$. We will not attempt to calculate the value of C_M and C_N, which depend on a much more detailed parametrization of the binding and interaction strength. A phenomenological examination

of the proton is given in Appendix B. Predictions for the neutron form factor, which depend sensitively on the symmetry of the nucleon wave function, are presented in Appendix C.

We can also apply these ideas to the many-quark bound system, $n=3A$, $A=2,3,\ldots$, which are the atomic nuclei. Two simple models for calculating the form factor of the six-quark deuteron are compared in Fig. 2. The simple democratic-chain model is shown in Fig. 2(a), again giving the form-factor results, Eqs. (30) and (34) with $n=6$. Note that in the case of color SU(3), where the gluon is a color octet, single-gluon exchange between the color-singlet nucleons is forbidden. However, if there is also an interchange of quarks between the nucleons then the color selection rules are satisfied. Thus the effective nucleon-nucleon potential is maintained as a color singlet.[16]

A somewhat more natural approach to the deuteron form factor is to recognize the two-nucleon nature of the deuteron, as in Fig. 2(b). In the limit of zero nucleon binding, each nucleon must move from $p/2$ to $(p+q)/2$ but stay intact; thus $F_d(q^2)$ should be proportional to $F_N^2(q^2/4)$. A representative diagram which explicitly displays this scaling is shown in Fig. 2(b). The momentum transfer $q/2$ to the second nucleon occurs immediately on the struck-quark line; a subsequent quark interchange satisfies the color rules. The struck quark recoils with momentum $p/6+q$, and its propagator gives the contribution of $(1-\frac{5}{6}q^2/\beta^2)^{-1}$ to the form factor. The deuteron form factor calculated in this way is

$$F_d(q^2)\sim \frac{F_p^{\,2}(q^2/4)}{(1-q^2/\frac{6}{5}\beta^2)}\,. \tag{37}$$

The most critical prediction is that the reduced form factor $f_d(q^2)\equiv F_d(q^2)/F_p^{\,2}(q^2/4)$ falls as $1/q^2$.[5] It is also interesting to note that the mass parameter $\frac{6}{5}\beta^2=0.28$ GeV^2 can be predicted from the pion-form-factor parametrization. A comparison of theory and experiment using both approaches is given in Sec. IV.

From a more general point of view the structure of the deuteron form factor at the quark level consists of three dynamical factors:

1. the generalized Compton amplitude on one nucleon

$$\mathfrak{M}^{\mu\nu}[\gamma(q)+N(p/2)\to g(q/2)+N'(p/2+q/2)],$$

2. a gluon propagator $\Delta(q/2)$, and
3. the form factor to absorb the gluon on the second nucleon. If the photon and gluon interact on the *same* gluon line then it is obvious that $\mathfrak{M}^{\mu\nu}$ contains the factor $F_N(q^2/4)$ and Eq. (37) follows. In fact, one does expect that the graphs with the gluon and photon on the same quark line will play a dominant role in $\mathfrak{M}^{\mu\nu}$ since this contribution gives interactions using immediately the leading Regge behavior ($j=0$ fixed pole) at large t. However, it should be emphasized that all of the Born terms contribute to the $(q^2)^{-5}$ asymptotic behavior.

It should be noted that the diagram in Fig. 2(b) can be regarded as the prototype for meson-exchange currents. At lower q^2, where coherent exchanges of gluon interactions can bind the quark lines to form virtual meson states, the quark approach merges with conventional calculations of the meson-exchange currents.[17] However, previous calculations using the meson degrees of freedom have predicted a deuteron form factor at large q^2 far in excess of experiment.[18] Other approaches, using vector dominance and subsequent multiple scattering, also fail in the comparison.[19] In common with Fig. 2(b), these calculations explore mechanisms which share the transferred momentum q equally to the deuteron's two nucleons. However, the meson-current calculations have not included the required off-shell vertex form factors at the meson-nucleon vertices. These must fall at least as fast as $F_N(q^2/4)$, as is immediately evident in the quark calculations.[20] Thus the short-distance behavior of nucleon interactions dictated by the quark model supplies the missing constraints of the previous hadronic level calculations. An explicit synthesis of these approaches is clearly needed.

The second approach contained in Fig. 2(b) and Eq. (37) can be generalized for heavier nuclei by counting nuclei connected by the gluon interaction and one or more quark interchanges. For example, the model applied to helium is displayed in Fig. 5. The diffractive behavior observed in the charge form factors of the He nuclei for $q^2=0.8$ GeV^2 should yield and eventually fall at large q^2 as

$$F_{^3\mathrm{He}}\sim F_p^{\,3}\left(\frac{q^2}{9}\right)\frac{1}{(1-q^2/\frac{9}{8}\beta^2)(1-q^2/\frac{27}{10}\beta^2)} \tag{38}$$

and for the α particles as

$$F_{^4\mathrm{He}}\sim F_p^{\,4}\left(\frac{q^2}{16}\right)\times\frac{1}{(1-q^2/\frac{12}{11}\beta^2)(1-q^2/2\beta^2)(1-q^2/\frac{24}{5}\beta^2)}\,. \tag{39}$$

At very large q^2, Eqs. (38) and (39) reduce to $F_n\sim(q^2)^{1-n}$ in agreement with the dimensional counting rules. Further, the results are consistent with the counting rule $f_A\sim(q^2)^{1-A}$ for the reduced form factor of the composite nuclear system as discussed in Sec. II B and summarized in Table I. We do not attempt to predict the normalization here.

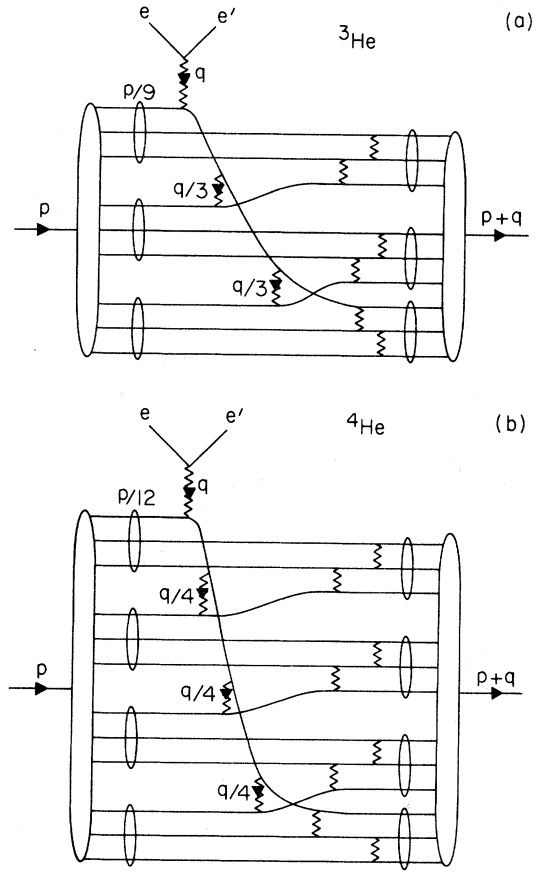

FIG. 5. Equipartition of q^2 for e-^{3}He and e-^{4}He elastic scattering at large momentum transfers.

III. DATA SET

For the π, p, n, and d particles of spin, 0, $\frac{1}{2}$, $\frac{1}{2}$, and 1, respectively, consistent form factors will be extracted from the scattering cross sections in order to compare the functions $(q^2)^{n_H-1}F_H$ for $n=2$, 3, and 6. In accord with Eq. (13), we use $F_H=A_H^{1/2}$, where A_H is the elastic electromagnetic structure function of the hadron's bound state.

A. Pion

The pion form factor is taken from the electroproduction work of the Harvard and Cornell collaboration for the reaction $e^-+p\to e^-+\pi^++n$ in the interval $0\leq -q^2\leq 4$ GeV^2.[15] This group measured the π^-/π^+ ratio from deuteron electroproduction in order to remove the small isoscalar component of the primary isovector pion form factor. Their resulting fit to the data is

$$F_\pi=\frac{1}{1-q^2/0.47}\ . \tag{40}$$

The pion data set has 16 values. In the timelike region F_π has been measured by the reaction $e^+e^-\to\pi^+\pi^-$ for $q^2\leq 9$ GeV^2.[21]

B. Proton

The proton form factors have been extensively studied since 1957 and span the interval $0\leq -q^2\leq 33$ GeV^2. The spin-$\frac{1}{2}$ proton has two electromagnetic form factors, G_{Ep} and G_{Mp}. The form factor G_{Ep} dominates only near $q^2\sim 0$ and is negligible for $-q^2\geq 3$ GeV^2. This form factor has not been separated beyond this point. We will use the proton structure function $A_p(q^2)$ from the measured cross sections

$$\frac{d\sigma}{d\Omega}=\left(\frac{d\sigma}{d\Omega}\right)_{\text{Mott}}[A_p(q^2)+B_p(q^2)\tan^2\tfrac{1}{2}\theta_e]\ , \tag{41}$$

where $B_p(q^2)=2\tau G_{Mp}^2(q^2)$, $\tau=-q^2/4M_p^2$, and θ_e is the laboratory angle. For $-q^2>3$ GeV^2, the empirical relation $G_{Ep}=G_{Mp}/\mu_p$ is used to determine $A_p(q^2)$, where μ_p is the proton's magnetic moment. In terms of G_{Ep} and G_{Mp}, the structure function is

$$A_p(q^2)=\frac{G_{Ep}^2+\tau G_{Mp}^2}{1+\tau} \tag{42}$$

and in the large-q^2 limit

$$A_p\simeq G_{Mp}^2\ . \tag{43}$$

The normalization is $A_p(0)=1$. The proton's form factor is

$$F_p(q^2)=\sqrt{A_p}\ . \tag{44}$$

Five overlapping sets of data are chosen from the literature with 43 measured values of the ep elastic scattering cross sections in order to determine $F_p(q^2)$ in the 0–33 GeV^2 interval.[22] Further data on G_{Ep} measurements or limits have been added to study the A-B connection of Eqs. (14), (15), and (16).[23] The empirical dipole fit,

$$G_{Mp}=\frac{\mu_p}{(1-q^2/0.71)^2}\ , \tag{45}$$

describes the data to within ~5% accuracy in the interval 0–7 GeV^2 and to within 20% accuracy out to $-q^2=33$ GeV^2. Timelike data for the proton form factors from $e^+e^-\to p\bar{p}$ exist only for $q^2=4.4$ GeV^2 with limits set at 5.1 and 6.8 GeV^2.[24]

C. Neutron

The neutron's charge form factor has been measured in the interval $0\leq -q^2\leq 2.7$ GeV^2 using two techniques, elastic and quasielastic eD scattering. The former reaction determines $(G_{Ep}+G_{En})^2$ and the latter G_{En}^2 and G_{Mn}^2. We note that at large q^2, where relativistic and model effects become important, the validity of using the elastic form fac-

tor of the deuteron to obtain the neutron form factor becomes suspect. The form factor G_{Mn} dominates the neutron structure function, $A_n(q^2)$.[25] Since the relation

$$G_{Mn} \cong \mu_n \frac{G_{Mp}}{\mu_p} \tag{46}$$

is observed to describe the existing neutron data, the q^2 dependency of $F_n(q^2)$ will be the same as $F_p(q^2)$ of Eq. (44) out to $-q^2 = 2.7$ GeV^2.

D. Deuteron

The deuteron data are from the recent measurement of ed elastic scattering in the range $0.8 \leq -q^2 \leq 6$ GeV^2.[1] This work extended information on the deuteron from the previous boundary at $q^2 = 1.3$ GeV^2. Thirteen data from lower-q^2 measurements are added to complete this data set.[26] The invariant structure function $A_d(q^2)$ as in Eq. (41) for the proton determines the deuteron form factor, $F_d(q^2) = \sqrt{A_d}$, where $A_d(0) = 1$. The deuteron structure function for this spin-1 particle is the sum of the squares of three invariant form factors which in the low-q^2 limit represent the distributions of charge, quadrupole moment, and magnetic moment, respectively. However, as shown in Sec. II A, it is $F_D(q^2)$ which contains the full dynamics of the deuteron for a large-q^2 collision.

Having described the data sets for the π, p, n, and D and the choice of consistent electromagnetic form factors for these spin-0, $-\frac{1}{2}$, and -1 particles, we now examine the scaling behavior of this set.

IV. SYSTEMATICS OF FORM FACTORS

In order to compare experiment and theory, we first examine the elastic form-factor data in the dimensional-scaling quark model (DSQM) whose domain of validity is the large-q^2 limit, i.e., $q^2 \gg M^2$. Next the data are compared with the refinements to this model developed in Sec. II D to include binding corrections and therefore connect the DSQM to lower q^2. Then the quark-interchange refinements are applied to the nuclei, ^{2}H, ^{3}He, and ^{4}He. Finally the connection between the elastic electromagnetic structure functions $A(q^2)$ and $B(q^2)$ is compared with our predictions of Sec. II A.

A. DSQM

The dimensional-scaling quark-model predictions for elastic form factors are applied to the pion, proton, neutron, and deuteron data and are presented in Fig. 1. We use Eq. (5) to test scaling by plotting the data as the quantity

$$(q^2)^{n-1} F_n \ , \tag{47}$$

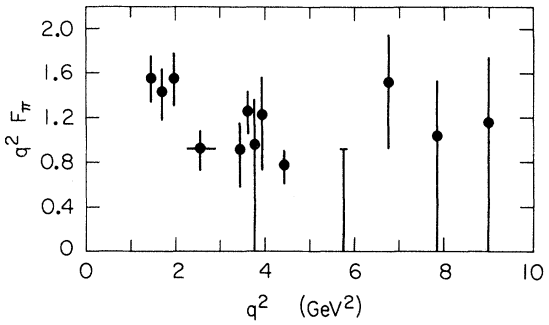

FIG. 6. Pion data for $q^2 > 0$ from $e^+e^- \to \pi^+\pi^-$.

where n is the number of quarks.

The principal observations in Fig. 1 are the known scaling (q^2 independence) for the pion, the approximate q^2 independence for the proton, and the approach to scaling observed for the neutron and the deuteron. Thus the quantity in Eq. (47) is an asymptote. The proton data have previously been displayed out to $-q^2 = 25$ GeV^2 (see Appendix B) and the pion data for timelike q^2 out to 9 GeV^2.[3] The more recent pion data for $q^2 > 0$ are displayed in Fig. 6 and observed to scale. Timelike data for the proton are too scant to examine.

In Fig. 7 these same data of Fig. 1 are superimposed on a linear scale. Scaling of the pion and proton form factors is observed beyond $-q^2 = 2$ and 6 GeV^2, respectively. The observation of a universal behavior for hadrons is suggested here

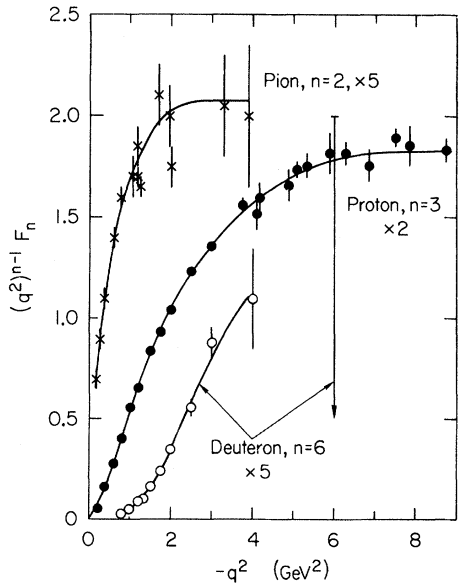

FIG. 7. Pion, proton, and deuteron data of Fig. 1 (multiplied by 5, 2, and 5, respectively) displayed on a linear scale.

since the deuteron form factor displays the same shape in the *approach to scaling* as do the pion and proton. It had been predicted that the deuteron would scale at higher q^2 (≥ 8 GeV^2) than the limits of the data.[3] The deuteron curve in Fig. 7 for $n=6$ will fit approximately on top of the proton curve for q^2 (deuteron) ≥ 2 GeV^2 if it is displaced toward lower q^2 by 1.5 GeV^2. This displacement would extrapolate to deuteron scaling at $-q^2 \simeq 6+1.5=7.5$ GeV^2. The value of n in Eq. (47) can be varied to see whether the resulting deuteron curve fits the proton shape. The value $n=5$ is unlikely since the deuteron curve would flatten (scale) already at 3 GeV^2, which is much earlier than the observed proton scaling. The deuteron data approximately fit the proton shape for $n \cong 6 \pm 0.6$. We shall await the final analysis of the large-q^2 deuteron data in order to make a more quantitative statement.

These observations in Figs. 1 and 9 using the DSQM prediction in Eq. (5) suggest that the neutron and deuteron are approaching scaling. The neutron data will not be analyzed further because of their restricted q^2 range. Neutron scaling predictions for large q^2 are presented in Appendix C.

B. Binding corrections to DSQM

We next examine the present refinements to the DSQM in Sec. II D to see whether scaling occurs at lower q^2 as in deep-inelastic scattering. The asymptotes using Eq. (30) are computed for the data set and are presented in Fig. 8. *Scaling is observed to appear for the π and proton form factors at lower q^2 than in Figs. 1 and 7.* This is similar to the behavior of the inelastic structure functions, νW_2 and W_1, when studied versus the variable ω' or ω_s rather than ω.[7] Scale independence sets in immediately (versus 2 GeV^2 in Fig. 9) for the pion as is obvious comparing Eqs. (32) and (40) and at $-q^2=4$ GeV^2 (versus 6 GeV^2 in Fig. 7) for the proton. Moreover, the proton appears to be asymptotic out to the experimental boundary, $-q^2=33$ GeV^2 (see Appendix B and Figs. 12 and 13) and thus represents a benchmark for the scaling behavior of elastic form factors. The upper dashed curve for the deuteron data in Fig. 8(c) is consistent with Eq. (37) while the lower dashed curve goes through the error bars at $-q^2=3$ and 4 GeV^2. Larger-q^2 data are needed to confirm what is only a suggested flattening out of this deuteron curve in Fig. 8.

We remark that the approximate asymptote from Eq. (34), i.e.,

$$\left(1-\frac{q^2}{m_n^2}\right)^{n-1} F_n, \quad m_n^2 = n\beta^2 \tag{48}$$

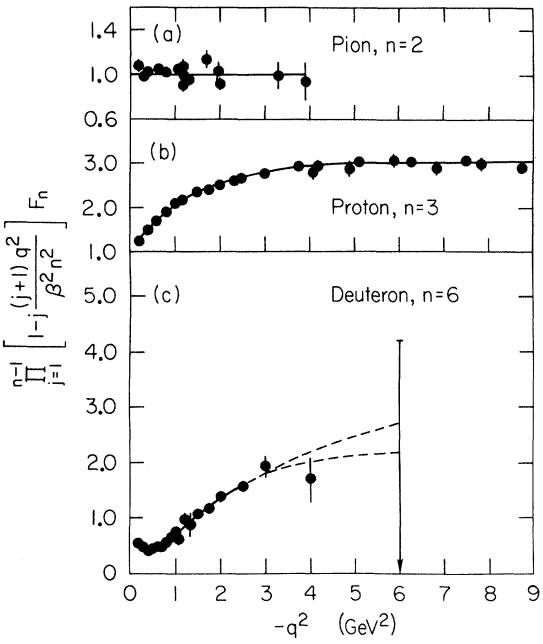

FIG. 8. The elastic form factors with the DSQM refined to include possible binding corrections given by Eq. (30). The curves connect the data points and the dashed curves in (c) are explained in the text.

reproduces the main features of Fig. 8. The mass parameter for $n=6$ is $m_n^2=1.41$ GeV^2. For the deuteron data set a change in slope occurs at $-q^2 \simeq 0.7$ GeV^2 after falling with q^2 up to this area of inflection which probably indicates that the asymptotic region begins here.

C. Quark-interchange DSQM

Next the deuteron data are examined by the constituent-interchange model of Fig. 2(b). The deuteron's asymptote for the quark-interchange prediction contained in Eq. (37) is presented in Fig. 9. In Eq. (37) the effective mass is taken from the pion form factor so that $\frac{6}{5}\beta^2=0.282$ GeV^2; the nucleon form factors are evaluated at $q^2/4$ using the dipole in Eq. (36) [and (45)]. Evaluating F_p using Eq. (33) does not change the features in Fig. 9 and using a larger effective mass, $\frac{6}{5}\beta^2 \approx M_p^2$, has only a minor effect on the resulting asymptote.[1]

The flattening of the curve in Fig. 9 at $-q^2 \sim 0.7$ GeV^2 is striking and is evidence for the validity of the underlying $(q^2)^{-5}$ behavior of the deuteron form factor as predicted by the DSQM in Eq. (5). Four powers of q^2 come from the two nucleons and the fifth power from the extra quark propagator, assuming a scale-invariant interaction. This observation lends support to viewing the deuteron at short distances by means of Fig. 2(b). Comparison of Figs. 3 and 9 supports our view of the determin-

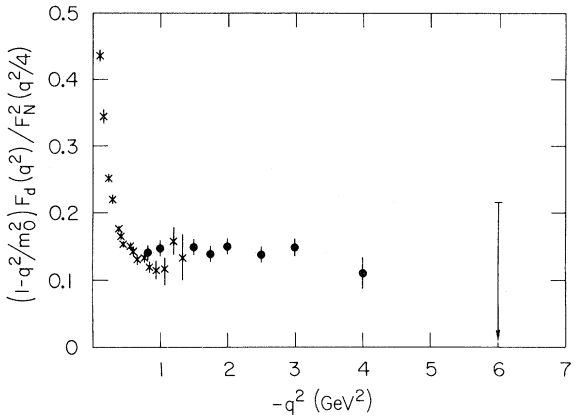

FIG. 9. Deuteron form factor divided by the quark-interchange prediction of Eq. (37). The data are from Ref. 26 (×) and Ref. 1 (●).

ation of compositeness, since the reduced deuteron form factor from Eq. (18) with $A=2$ is $f_D \sim 1/q^2 \sim F_\pi$.

Further, the magnitude of the asymptote in Fig. 9 can be estimated or used to determine $\psi_D(0)$ together with large-transverse-momentum np elastic scattering data as in Eq. (26).

D. Helium form factors

We can apply these ideas to the elastic form factors of ^{3}He and ^{4}He, using the predictions of Eqs. (38) and (39) from constituent interchange, as in Figs. 2(b) and 5. However, the presently measured elastic electron scattering data on both nuclei extend only to $-q^2=0.8$ GeV^2 with diffraction minima observed at ~0.4 GeV^2, followed by large secondary maxima.[27] If these diffractive features of the nucleon-nucleon repulsion yield to the quarklike short-distance behavior by $-q^2 \sim 2$ GeV^2, then we should be able to predict the asymptotic cross sections from the systematics developed in this paper.

The upper curves in Fig. 10 for $-q^2>1$ GeV^2 are our predictions for ^{3}He and ^{4}He. We can predict the q^2 dependence of these form factors but the magnitudes can only be estimated. That is, the curves in Fig. 10 assume that scale-invariant behavior begins at $-q^2 \simeq 1$ GeV^2. Should this momentum dependence begin, for example, at $-q^2 \simeq 1.2$ GeV^2, then our curves would be a factor ~2.5 too high. The crucial predictions are the underlying $(q^2)^{-8}$ and $(q^2)^{-11}$ behavior as embodied in Eqs. (38) and (39) or, equivalently, that the reduced helium form factors from Eq. (18) for $A=3$ and 4 diminish as $1/(q^2)^2$ and $1/(q^2)^3$, respectively. Large-momentum-transfer data on ^{3}He and ^{4}He would be welcome to test these ideas.

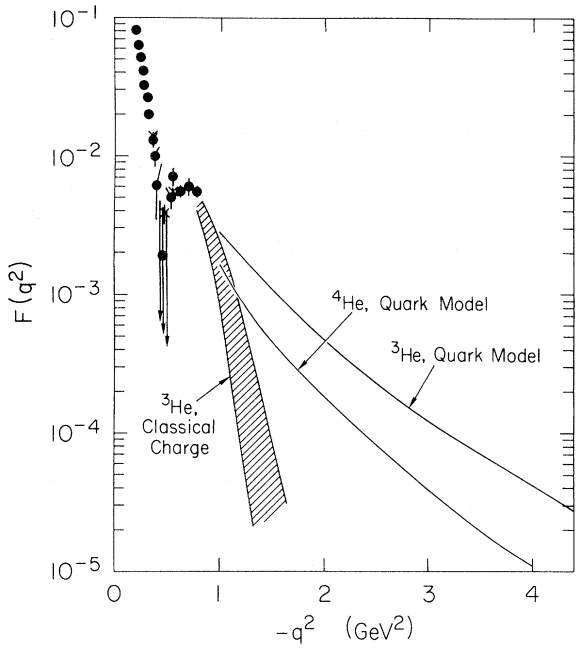

FIG. 10. ^{3}He and ^{4}He data and an estimate for large q^2 using Eqs. (38) and (39). A smooth normalization at $(q^2) \sim 1$ GeV^2 is assumed. The data are from Ref. 27.

E. A-B connection

In relating fixed-angle scaling laws to electromagnetic form factors in Sec. II A, a connection between the structure functions $A(q^2)$ and $B(q^2)$ was derived and summarized by Eqs. (14), (15), and (16). The quantity $(-q^2/2M^2)A/B$ is predicted to approach unity for spin-$\frac{1}{2}$ constituents or $(1+R)/(1-4M^2/q^2)$ using Eq. (16). The available data[23] for the proton, where G_{Ep} and G_{Mp} have been separated, is presented in Fig. 11. A phenomenological fit to the proton, which is discussed in Appendix B, is used to extrapolate to large q^2 in Fig. 11(b). The proton data are suggestive, but of too small q^2 to test these predictions. Accordingly, measurements or limits at large q^2 of B/A would be useful. B/A data exist for the deuteron and ^{3}He, but only for $-q^2 \lesssim 1$ GeV^2 (see Ref. 28).

V. SUMMARY OF RESULTS

Elastic form factors of hadrons have been systematically examined from the viewpoint of the dimensional-scaling quark model. This theory ascribes the power-law behavior in q^2 observed for the pion and the proton to the number of internal degrees of freedom. The large-q^2 behavior of the quantity $(q^2)^{n-1}F_n$ appears to be asymptotic or approaching this condition for the π, p, n, and D data sets as summarized in Fig. 1.

Three new results for elastic form factors are derived in Sec. II for the large-q^2 limit. Comparing fixed-angle scaling laws with the Rosenbluth equation for elastic electron scattering, we find for the measured structure functions of A $+B\tan^2\frac{1}{2}\theta_L$ that

$$F_H = A^{1/2}(t)$$

and

$$B(t) \to \frac{-t}{2M^2} A(t)$$

reflects the dynamics of spin-$\frac{1}{2}$ constituents. An equipartition model for general systems with a series of scales of compositeness of A constituents leads us to define a reduced form factor $f_A(t)$ by removing the structure of the constituents as in Eq. (17); then

$$f_A(t) \sim \text{const}/t^{A-1}.$$

As shown in Secs. III and IV and in Fig. 13, the definition of the large-q^2 hadronic form factor $F_H(t)$ is consistent with the full dynamics of a bound state recoiling at large q^2. The A-B connection above would appear to be consistent with the proton form factors, as in Fig. 11. G_{Ep} and G_{Mp} separations at $-q^2 > 3$ GeV^2 are very difficult but possible by high-precision angular distributions at fixed q^2 and polarized-beam–polarized-target methods. Even limits on B/A at large q^2 would be useful. Preliminary results for B/A for the deuteron are interesting.[28]

The general working principle for composite systems is summarized by predictions for the reduced form factor $f_A(t)$ in Table I. It has been verified for elementary bound states up to the lightest atomic nucleus, the deuteron in Figs. 3 and 9. The reduced form factors of ^{3}He and ^{4}He are predicted to diminish as t^{-2} and t^{-3}, respectively. Dimensional-scaling predictions are made in Eq. (29) for the quark, if it too is eventually determined to have substructure.

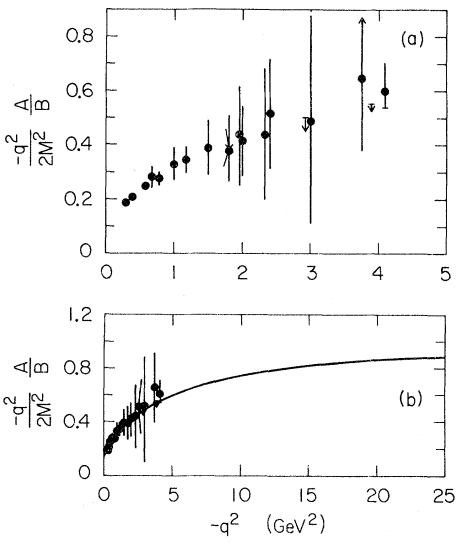

FIG. 11. A-B connection for proton form factors.

Simple models have been explored which extend the dimensional-scaling quark model to lower q^2 by retaining binding-energy corrections to the leading fermion propagator. The mass scale of these corrections is set by the constant in the measured pion form factor with $2\beta^2 = 0.47$ as in Eqs. (32) and (40). It is encouraging that this mass scale gives the well-known empirical value for the nucleon form factors, i.e., $3\beta^2 = 0.705$ GeV^2. Thus the empirical dipole fit to the proton and neutron form factors, which has been a long-standing curiosity, is observed to arise from two off-shell fermion lines using a mass scale set by the pion form factor. The mass, $\langle\beta^2\rangle^{1/2} = 0.485$ GeV, may be related to a universal mean transverse momentum. This value is in accord with other high-energy phenomenology.

Furthermore, with these refinements to the DSQM, scaling for the pion and proton is observed to occur at lower q^2, as in Fig. 8, compared for example with Fig. 7. This effect of early scaling is reminiscent of the situation in deep-inelastic scattering and is therefore suggestive of a further link between exclusive and inclusive scattering.

The approach of the deuteron form factor to the scaling limit $(q^2)^{-5}$ was the impetus for the present work. The intimate connection to n-p elastic scattering at fixed angle led to three especially interesting results in Sec. II C.

1. The large-q^2 falloff of the deuteron form factor predicted from np scattering is determined to be $(q^2)^{-4.85\pm0.25}$. This is consistent with dimensional scaling and a six-quark deuteron.

2. The deuteron form factor, together with the measured np cross section, fixes the deuteron wave function at the origin, leading to $u'(0) \sim 0.1 m_\pi^{3/2}$.

3. The effective nucleon-nucleon potential diminishes as $(q^2)^{-4}$ so that its entire behavior is due to the dynamical structure of the nucleons with no additional q^2 structure from the exchange force.

The large-q^2 deuteron form factor has been examined from two simple models displayed in Fig. 2, the democratic chain model [Fig. 2(b)], and the quark-interchange model [Fig. 2(b)]. Figure 8 displays the rapid approach of F_D to scaling given the validity of this chain or cascade model. In support of the interchange model, it is observed in Fig. 3 that the reduced deuteron form factor f_d indeed approaches $(q^2)^{-1}$. We believe that the simplicity of this result is remarkable. Binding

corrections are calculated which modify the result to $f_d \sim (1 - q^2/\frac{6}{5}\beta^2)^{-1}$, and the ratio of experiment to theory in Fig. 9 appears to be independent of q^2 beyond 0.7 GeV^2. Further consistency with the np data (item 2 above) gives an estimate of the magnitude of the observed asymptote. It is emphasized that the quark-interchange model provides a viable mechanism to transfer momentum q/N to each of N nucleons which has been the goal of meson-exchange-current calculations for the last decade. As such, the prediction in Eq. (37), which may be written as

$$F_d \sim F_p^2(q^2/4)F_\pi(5q^2/3)\,, \tag{49}$$

may be a useful guide. Stating this point more strongly, it is our belief that the interactions displayed in Figs. 2(b) and 5 are prototypes for equipartition of momentum among nucleons at large q^2.

The possibility of distinguishing between the two models of Fig. 2 is displayed by dashed-line extrapolations beyond $-q^2 = 4$ GeV^2 in Fig. 8. That is, will larger-q^2 data on $A_d(q^2)$ for $-q^2 \gtrsim 4$ GeV^2 favor the upper dashed curve, which is from Fig. 2(b), i.e., constituent interchange, or is the deuteron already scaling at $-q^2 \gtrsim 4$ GeV^2? Plausible differences could give a factor of ~3 in cross section at $-q^2 = 6$ GeV^2 and a factor of ~6 at 8 GeV^2. The principal issues would appear to be

a whether it is possible to distinguish which model in Fig. 2, democratic chain or constituent-interchange, better describes the turn-on of scaling,

b whether the internal rearrangements required by the color-singlet nature of two hadrons as in Fig. 2(b) are a viable description of the deuteron at short distances, and

c what is the magnitude of the deuteron wave function $\psi_d(0)$? For the evaluation in Eq. (27), the value used for $(q^2)^5F_d$ came from the upper dashed curve in Fig. 8. The calculations need to be refined to include spin effects, etc.

It is pointed out in Sec. IV that diffractive features dominate the ^{3}He and ^{4}He form factors out to the experimental boundaries at $-q^2 = 0.8$ GeV^2. If $n = 9$ and $n = 12$ quarks are the origin of the short-distance behavior of these nuclei, then the diffractive behavior should yield to the asymptotic decreases in F_n at larger q^2, as predicted in Table I and by Eqs. (38) and (39) with an estimate given in Fig. 10. Otherwise our conjectures will have to be revised in order to account for the possible dominance of diffractive behavior at large q^2. Future experiments will provide the guidance.

Clearly work remains to be done in several areas. The success and simplicity of the weak-binding approximation employed in Ref. 3 has to be fully understood. A more careful treatment of the Bethe-Salpeter bound state, which permits the mass scale to enter at a more fundamental level, and the universality of a mean transverse momentum on the propagator should be investigated. The normalizations of the form factors are of fundamental significance in representing the wave function at $x_\mu = 0$ and should come naturally out of a successful theory of hadronic structure. The present explorations using consistency with np scattering cross sections should be elaborated. It is very important to understand more about the spin structure of the gluon interaction. Although the scaling behavior is not changed, different renormalizable field theories will affect nonasymptotic terms.

Experiments at larger momentum transfer and those with improved statistical accuracy will provide decisive answers to whether scale invariance is exact in the case of the proton. Are logarithmic corrections visible with precise data? We discuss the large-q^2 proton data in Appendix B, in particular examining which form factor scales: F_p, F_{1p}, or G_{Mp}. The issue of scale breaking has been discussed from several other points of view.[14] More data on the hadron form factors in the timelike region from $e^+e^- \to \pi^+\pi^-$, K^+K^-, $p\bar{p}$, $n\bar{n}$, $d\bar{d}$, etc., will test the crossing symmetry of the dimensional-scaling quark model. Deuteron data at larger q^2 will determine whether the scaling observed in Fig. 8 is illusory. Extensions of the neutron form factors to larger q^2 would determine the isotopic differences in the nucleon at $x_\mu = 0$ and complement the νW_2 differences in deep-inelastic scattering. Predictions for the neutron and n/p are given in Appendix C. Finally, the extension of the ^{3}He and ^{4}He form factors to larger q^2 would have direct bearing on the ideas we have advanced and in particular test whether nuclei are simply many-quark systems at short distances.

VI. CONCLUSION

The deuteron form factor $F_d(q^2)$ provides an ideal illustration of the continuity between nuclear and particle physics at the microscopic level. At low momentum transfers, where the nucleons can be treated as pointlike objects and are the essential degrees of freedom, the usual effective-potential Schrödinger theory is appropriate and meson-exchange effects provide the framework for the nuclear interaction. However, at larger momentum transfers, where the nucleon form factor differs significantly from its $q^2 = 0$ value, hadronic substructure comes into play, and the electromagnetic interaction begins to resolve an elementary fermion current; the quark degrees of freedom then become appropriate. The elastic form

factor of the nucleus is equivalent to the probability amplitude to rearrange n elementary constituents; the dimensional-counting prediction $(q^2)^{n-1}F(q^2) \to \text{const}$ then follows assuming a scale-invariant theory.

Further, the nuclear potential (the irreducible kernel of the two-nucleon Green's function) can be reexpressed in terms of quark diagrams. In particular, at large momentum transfers, meson-exchange diagrams of the potential theory merge at the microscopic level with the quark-exchange diagrams (dual graphs). In Sec. II C we saw that the scaling of the deuteron form factor is in fact consistent with the observed power-law scaling behavior of the two-nucleon amplitude at $\theta_{\text{c.m.}} = 90^\circ$ (which can also be predicted using quark counting). As shown in Ref. 3 the angular distribution of the nucleon-nucleon scattering amplitude at large t and u agrees with that predicted by quark-interchange diagrams. We also emphasize that the empirical fixed-angle scaling behavior of the nucleon-nucleon scattering amplitude $\mathfrak{M}_{NN}^{(s,t)}/F_N^2(t) = f(\theta_{\text{c.m.}})$ implies that, after nucleon structure is removed, the nucleon-nucleon interaction is scale-invariant, as expected in theories without a fundamental length scale.

In this paper we have also noted the utility of defining reduced form factors which remove the structure of the constituents [see Eqs. (17) and (18)]. More generally, for any elastic nuclear reaction at large t $(aA \to aA)$ $(a = e,\ \pi,\ p,\ \text{etc.})$ it is useful to define the reduced scattering amplitude

$$\tau(aA \to aA) \equiv \frac{T(aA \to aA)}{\prod_{i=1}^{A} F_{N_i}(m_i^2/m_A^2 t)} , \tag{50}$$

which removes the effect of the probability amplitude for keeping the nucleons intact. The reduced amplitude $m(aA \to aA)$ then reflects the nuclear aspects of the scattering. Further, the ratio

$$R(aA \to aA) = \frac{T(aA \to aA)}{T(eA \to eA)} \tag{51}$$

effectively removes the falloff of the amplitude due to keeping the nucleus intact, and is the most sensitive test of the specific interaction of the projectile a, and is convenient for analysis of the validity of the impulse approximation at large momentum transfer.[29]

The methods discussed in this paper can also be applied to inelastic electron scattering on nuclei, below the energy for meson production. Following the parton-model analysis one derives (see Ref. 5)

$$\frac{d\sigma}{dt\,dx}(eA \to e'X) = \sum_{i=1}^{A} \frac{d\sigma}{dt}(eN_i \to eN_i) G_{N_i/A}(x) , \tag{52}$$

where $x = -t/2p_A \cdot q$ is the Bjorken variable $(0 < x < 1)$, $d\sigma/dt$ is the elastic electron-nucleon amplitude evaluated at the effective $s' = xs$, and $G_{N_i/A}(x)$ is the probability for the nucleon to have fractional momentum x in the $P \to \infty$ frame of the nucleus A. In a more general frame, $x = (p_N^0 + p_N^z)/(P_A^0 + P_A^z)$, where $\vec{P}_A$ is moving along the z direction. In the limit of zero binding energy $G \to \delta(x - 1/A)$, and Eq. (52) reduces to the usual quasielastic scattering formula. When nucleon interactions are allowed, a quasielastic peak still exists, but there is a finite tail (Fermi motion) which extends to $x < 1$. Using the quark-counting rules, one obtains for $x \to 1$

$$G_{N_i/A}(x) \propto (1 - x)^{6(A-1)-1} , \tag{53}$$

where $3(A-1)$ is the number of quark spectators in the reaction. This prediction could be tested by measurements in the forward fragmentation region of inelastic deuteron scattering, $d + A \to p + X$. This result also provides continuity between the exclusive and inclusive limits and the prediction,

$$\frac{d\sigma}{dt\,dW^2} = \left.\frac{d\sigma}{dt}\right|_{\text{elastic}} \rho(W^2) , \tag{54}$$

that the inelastic and elastic cross sections fall uniformly in t at fixed $W^2 = (q + p_A)^2$.

Note added in proof. The recent measurement of the reaction $e + d \to e' + X$ at threshold by the collaboration of Ref. 1 appears to support this prediction.[32]

ACKNOWLEDGMENTS

We are grateful to R. Arnold, R. Blankenbecler, G. Farrar, J. Gunion, I. Schmidt, and W. Schütz for helpful discussions and suggestions.

APPENDIX A: THE PARTITION METHOD FOR BOUND-STATE CALCULATIONS

There are many methods available for calculating the covariant amplitude for processes involving the scattering of composite states. These include Bethe-Salpeter analyses and Fock-space calculations in the infinite-momentum frame. Perhaps the simplest method is the "partition" method discussed in Ref. 3, which is particularly convenient for analyzing the scaling behavior of amplitudes, and also for proving cancellations in the infrared region for neutral systems. In the Bethe-Salpeter formalism one can replace each hadron with 4-momentum p by a cluster of n constituents each with momenta $p_i = \alpha_i p + \kappa_i$ $(i = 1, \ldots, n)$, where the α_i are fixed fractions satisfying

$$\sum_{i=1}^{n} \alpha_i = 1, \quad \sum_{i=1}^{n} \kappa_i = 0 .$$

The elastic scattering amplitude for $A+B \to C+D$ then takes the form

$$\mathfrak{M} = \int \prod_i d^4\kappa \, \psi_C^+ \psi_D^+ \mathfrak{M}_n \psi_A \psi_B \ ,$$

where $\mathfrak{M}_n$ is the corresponding connected multiparticle scattering amplitude and $\psi(\kappa_1, \kappa_2, \ldots, \kappa_{n-1})$ is the Bethe-Salpeter wave function.

Note that in the zero-binding limit we must have

$$\alpha_i \to m_i/M_T \ ,$$

$$\kappa_i \to 0$$

since in the rest frame $p_i \to (m_i/M_T)p = (m_i, \vec{0})$. In fact, if the binding interactions of a composite system are sufficiently well behaved, then at large momentum transfers binding corrections can be ignored and, effectively, the bound-state scattering amplitude is proportional to the on-shell multiparticle amplitude $\mathfrak{M}_n$ obtained by partitioning the momentum of each hadron among its constituents. The required condition for this to be valid is that the Bethe-Salpeter wave function be finite for all relative $x_\mu \to 0$, i.e., so that the integrations over the relative momentum are finite

$$\psi(x=0) = \int \prod_{i=1}^{n-1} d^4\kappa_i \psi(\kappa_i) < \infty \ .$$

This method is equivalent to iterating the Bethe-Salpeter equation and exposing the interaction kernel whenever large momentum transfer is required. In the case of spin, $\mathfrak{M}_n$ includes the on-shell Dirac spinor. In general, $\psi(x=0) < \infty$ is required for the bound state to lie on a Regge trajectory. This condition can also be derived in a renormalizable field theory with asymptotic freedom, modulo calculable logarithmic corrections. Further discussions may be found in Refs. 3 and 10.

APPENDIX B: PROTON FORM FACTORS

Several additional remarks are in order about the proton form factors at large q^2 because this is the most thoroughly studied hadron. G_{Mp} is known to dominate the cross section for $-q^2 > 1$ GeV^2 and the quantity $q^4 G_M$ is believed to be asymptotic (i.e., scales) out to the experimental boundary at $-q^2 = 33.4$ GeV^2. The empirical dipole fit in Eq. (45) is known to be an approximate fit which underestimates the data by a few percent for $-q^2 < 5$ GeV^2 and then overestimates the data by ~10–20% for $-q^2 > 10$ GeV^2. The detailed structure of G_{Mp} can be tracked if one puts enough parameters into the fit. Recent efforts in this direction which have theoretical content appear to be interesting, and we compare the scaling of the proton in this context. In addition it is important, when more accurate large-q^2 proton data become available, to understand which form factor is expected to scale, i.e., F_p, F_{1p}, or G_{Mp}.

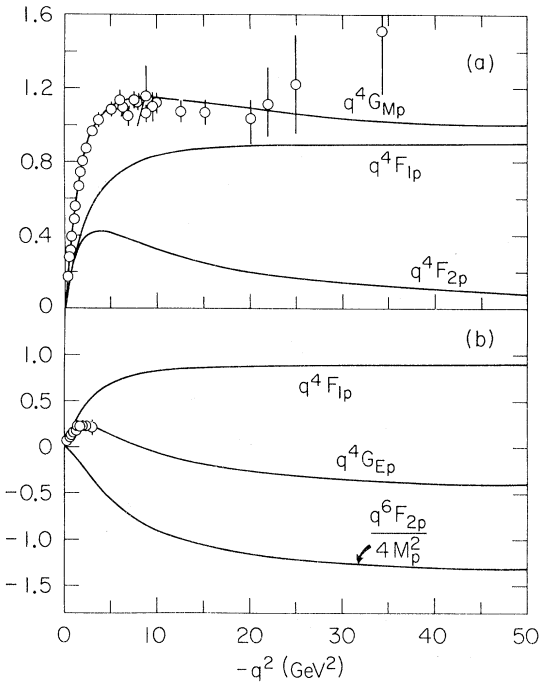

FIG. 12. Dimensional counting of proton form factors compared with a five-parameter semiphenomenological fit.

Semiphenomenological fits of Iachello, Lande, and Jackson (IJL)[30] are displayed in Figs. 12 and 13. The electromagnetic structure of the nucleon is represented in the IJL model by both direct and vector-meson couplings to the external photon. The resultant five-parameter dipole fit has a good $\chi^2 = 0.924$ for 112 data, as illustrated with representative data in Fig. 12 (see Ref. 31). However, the same phenomenology gives a poor fit to the neutron's, G_{Mn}. G_{Mn} is well described by the empirical dipole fit or Eq. (46).

The phenomenology in terms of the Dirac and

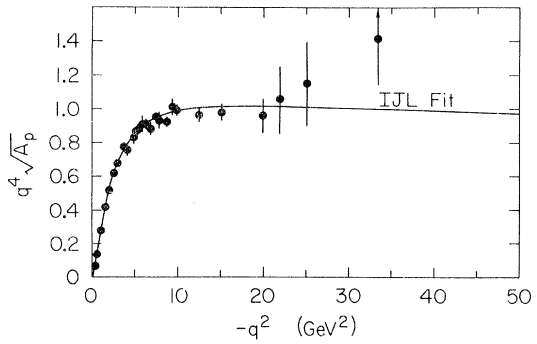

FIG. 13. The proton form factor $F_p = A^{1/2}$ compared with the IJL fit within the DSQM.

Pauli nucleon form factors is

$$G_{Ep} = F_{1p} + \frac{q^2}{4M^2} F_{2p} \ , \tag{B1}$$

$$G_{Mp} = F_{1p} + F_{2p} \ , \tag{B2}$$

where $F_{1p}(0) = 1$, and $F_{2p}(0) = 1.79$ is the proton's anomalous magnetic moment.

Three points are presented about the IJL fit to the data in Figs. 12 and 13:

1. It predicts that $q^4 F_{1p}$ scales exactly for $-q^2 > 20$ GeV^2, whereas $q^4 G_{Mp}$ will diminish by ~7% between $-q^2 = 10$ and 25 GeV^2. In other words, this implies that scaling for G_{Mp} should not be exact. Clearly only more accurate data would determine this question.

2. The IJL fit to $q^4 G_{Ep}$ is acceptable over the small region of existing data. There is little hope to separate G_{Ep} at much larger q^2; accordingly, $q^6 F_{2p}$ displayed in Fig. 12, which the IJL fit indicates will scale approximately for $-q^2 \gtrsim 25$ GeV^2, cannot be tested experimentally.

3. The quantity $q^4\sqrt{A_p}$ scales as illustrated in Fig. 3, where the data and the IJL fit are displayed. Use of the proton form factor, $\sqrt{A_p}$, in this work is discussed in Secs. II and III and defined in Eqs. (41)–(44). These observations are in accord with the specific three-quark model calculation of Ref. 3 for the proton, namely, $F_{1p} \sim (q^2)^{-2}$, $F_{2p} \sim F_{1p}/q^2$, and $G_{Ep}/G_{Mp} \sim$ constant, all at large q^2. However, note that the existing data are sensitive to only the first observation, $q^4 F_{1p} \sim$ constant at large q^2.

APPENDIX C: THE NEUTRON FORM FACTOR

The asymptotic form factor of the neutron, which can be measured in deuteron electrodisintegration and possibly determined from eD elastic scattering, can be a sensitive test of the symmetry of the nucleon wave function. Asymptotically, we expect from dimensional counting

$$(q^2)^2 F_{1n}(q^2) \to C_{1n}, \quad (q^2)^3 F_{2n}(q^2) \to C_{2n} \ . \tag{C1}$$

However, if the up and down quarks have the same wave-function dependence in the nucleon then C_{1n} is proportional to the sum of quark charges and vanishes. $F_{1n}(q^2)$ is then presumably negligible at all q^2, and we have

$$G_{En}(q^2) \sim \frac{q^2}{4M^2} G_{Mn}(q^2) \to \frac{C_{En}}{(q^2)^2} \ . \tag{C2}$$

Alternatively, the observed behavior of the ratio $\nu W_2^n / \nu W_2^p$ at $x \to 1$ suggests that the down (up) quarks in the neutron (proton) dominate the wave function at large momentum transfer and $C_{1n} \neq 0$. In this case we expect that

$$F_{1n}(q^2)/F_{1p}(q^2) \to -\tfrac{1}{2} \ , \tag{C3}$$

where the sign is a crucial part of the prediction of this model.

---

*Research supported by the Energy Research and Development Administration.

†Research supported by the National Science Foundation under Grant No. MPS75-07325.

[1]R. Arnold *et al.*, Phys. Rev. Lett. 35, 776 (1975).

[2]J. Stack, Phys. Rev. 164, 1904 (1967).

[3]S. Brodsky and G. Farrar, Phys. Rev. Lett. 31, 1153 (1973); Phys. Rev. D 11, 1309 (1975).

[4]V. Matveev, R. Muradyan, and A. Tavkhelidze, Lett. Nuovo Cimento 7, 719 (1973).

[5]S. Brodsky, in *Proceedings of the International Conference on Few Body Problems in Nuclear and Particle Physics, Laval Univ., Québec*, 1974, edited by R. Slobodrian *et al.* (Les Presses de L'Université Laval, Quebec, 1975), p. 676.

[6]J. Gunion and L. Stodolsky, Phys. Rev. Lett. 30, 345 (1973).

[7]R. Taylor, in *Proceedings of the 1975 International Symposium on Lepton and Photon Interactions at High Energies, Stanford, California*, edited by W. Kirk (SLAC, Stanford, 1975), p. 679.

[8]For simplicity we ignore spin here; inclusion of the spin factors leads to the same results.

[9]See Ref. 3 for an analysis of the p-p data. The new large-t n-p elastic scattering data are similar. J. Stone *et al.*, Bull. Am. Phys. Soc. Ser II, 21, 70 (1976).

[10]The exceptional case is the Landshoff graphs, which involve multiple on-shell quark-quark scattering [P. V. Landshoff, Phys. Rev. D 10, 1024 (1974)]. These graphs can be excluded phenomenologically and possibly theoretically. For a discussion see Ref. 3 and D. Sivers, S. Brodsky, and R. Blankenbecler, Phys. Rep. 23C, 1 (1976). A recent derivation of dimensional counting for meson form factors in a renormalizable field theory is given by M. Goldberger, A. Guth, and D. Soper, Phys. Rev. D 14, 1117 (1976).

[11]We assume that the transition form factor is a function of $t + \mathfrak{M}^2$. See for example E. D. Bloom and F. Gilman, Phys. Rev. D 4, 2901 (1971).

[12]M. Moravcsik and P. Ghose, Phys. Rev. Lett. 32, 321 (1974).

[13]J. Harte, Phys. Rev. 165, 1557 (1969); J. Ball and F. Zachariasen, *ibid.* 170, 1541 (1968).

[14]M. Chanowitz and S. Drell, Phys. Rev. D 9, 2078 (1974).

[15]C. Bebek *et al.*, Phys. Rev. D 13, 25 (1976).

[16]*Note added in proof.* For a discussion of the suppression of the form factor from quark statistics for systems beyond 12 quarks, see de Franceschi, Palumbo, and Simonov (Ref. 32).

[17]R. Woloshyn, Phys. Rev. Lett. 36, 220 (1976).

[18]M. Chemtob, E. Moniz, and M. Rho, Phys. Rev. C 10, 334 (1974).

[19]R. Blankenbecler and J. Gunion, Phys. Rev. D 4, 718

(1971).
[20]For a use of phenomenological vertex form factors, see M. Gari and H. Hyuga, Phys. Rev. Lett. 36, 345 (1976).
[21]D. Bollini *et al.*, Lett. Nuovo Cimento 14, 418 (1975).
[22]Ch. Berger *et al.*, Phys. Lett. 35B, 87 (1971); W. Bartel *et al.*, Nucl. Phys. B58, 429 (1973); W. Albrecht *et al.*, Phys. Rev. Lett. 17, 1192 (1966); P. N. Kirk *et al.*, Phys. Rev. D 8, 63 (1973); W. Atwood, SLAC Report No. SLAC-185, 1975 (unpublished).
[23]W. Albrecht *et al.*, W. Bartel *et al.*, and Ch. Berger *et al.* in Ref. 22; K. Hanson *et al.*, Phys. Rev. D 8, 753 (1973); J. Litt *et al.*, Phys. Lett. 31B, 40 (1970); K. Chen *et al.*, Phys. Rev. 140, B1267 (1965).
[24]M. Gourdin, Phys. Rep. 11, 29 (1974). This review contains extensive references on nucleon form factors. For a recent review of the theory, see Ref. 10.
[25]W. Bartel *et al.* and K. Hanson *et al.* in Refs. 22 and 23, and R. Felst, DESY Report No. DESY 73/56 (unpublished).
[26]J. Elias *et al.*, Phys. Rev. 177, 2075 (1969), and Ref. 4 therein; S. Galster *et al.*, Nucl. Phys. B32, 221 (1971).
[27]The black dots in Fig. 10 are from measurements of J. McCarthy *et al.*, Phys. Rev. Lett. 25, 884 (1970); ×'s are from M. Bernheim *et al.*, Lett. Nuovo Cimento 5, 431 (1972).
[28]For the deuteron, the quantity $(-q^2/2M_D^2)A/B \simeq 0.4 \pm 0.1$, i.e., approximately constant over the limited measured range out to $-q^2 = 0.55$ GeV^2. A preliminary result by the collaboration of Ref. 1 gives B at $-q^2 = 1$ GeV^2 and the ratio is 0.69 ± 0.46. F. Martin (private communication).
[29]See, for example, S. Gurvitz, Y. Alexander, and A. Rinat, Weizmann Report No. WIS-75-19 Ph., 1975 (unpublished).
[30]F. Iachello, A. Jackson, and A. Lande, Phys. Lett. 43B, 191 (1973).
[31]Reference 30 was written before the final data of Bartel *et al.* (Ref. 22) and K. Hanson *et al.* (Ref. 23), but inclusion of these data and those of W. Atwood (Ref. 22) does not degrade the excellent χ^2 for the proton.
[32]W. Schütz *et al.*, SLAC Report No. SLAC-Pub-1770, 1976 (unpublished). For other recent theoretical work see L. L. Frankfurt and M. I. Strikman, Leningrad Reports Nos. LNPI-227 and 238, 1976 (unpublished); G. de Franceschi, F. Palumbo, and Yu. A. Simonov, Report No. LNF-76(P), 1976 (unpublished); and V. I. Zakharov, Report No. ITEP-127, Rapporteur talk at the XVIII International Conference on High Energy Physics, Tbilisi, 1976 (unpublished).